Dentistry 3000

Vol 14, No 2 (2026)
ISSN 2167-8677 (online)
DOI 10.5195/d3000/2026.1548

# Employing Cluster- and Threshold-Based Techniques for Lesion Interaction in Dental Radiography

**Doha Qasim, Rabab S. Abdoon**
*Department of Physics, College of Science, University of Babylon, Iraq*

**Open Access**
Citation: Qasim D et al. (2026) Employing Cluster- and Threshold-Based Techniques for Lesion Interaction in Dental Radiography. Dentistry 3000. 1:a001 doi:10.5195/d3000.2026.1548
Received: August 8, 2026
Accepted: August 11, 2026
Published: September 10, 2026

Email: doha.ibrahim511@student.uobabylon.edu.iq

## Abstract

An image-processing-based technique for identifying and segmenting lesion regions in dental X-ray images is described in this research. The low contrast of these images and the similarity in intensity between lesion sites and surrounding tissues continue to make accurate detection difficult. Image enhancement approaches first improve image quality and highlight the lesion spots to address this issue. To enhance the visibility of important features, this work employs preprocessing techniques such as contrast adjustment and histogram equalization. It differentiates the similar homogeneous areas in the image that use different segmentation techniques like K-means clustering, fuzzy C-means (FCM), etc. The paper aims at suggesting a hybridization of fuzzy C-means and histogram equalization to improve the accuracy of the segmentation process. The results showed that with all hybrid methods, the computation time was decreased compared to the FCM algorithm, while the accuracy for lesion detection increased. Morphological operations are furthermore used to improve the quality of the obtained segmentation and retrieve the area of interest. The experimental results on dental X-ray images demonstrate that the proposed method can successfully localize lesions and boost segmentation performance.

## Introduction

Dental panoramic radiography is one of the most important diagnostic imaging modalities in modern dentistry since it allows visualizing, in a single image, the teeth as well as the jaws and surrounding anatomical structures altogether. It is important in the diagnosis of a variety of dental diseases contributing to effective treatment planning and follow-up examinations (periapical lesions, cysts, tumors, impacted teeth, and detection of carious lesions). Panoramic radiography has established itself as an imaging modality within dentistry due to its large anatomical field of view and low radiation exposure [1,2]. Automatic analysis of panoramic dental radiographs is seldom employed due to the nature of X-ray images, lower quality, or even abnormal images, although valuable information carries important diagnostic advantages. Poor image qualities, including low contrast, noises, intensity inhomogeneity, blurred lesion boundaries, and overlapping anatomical structures, often reduce the identification of pathological regions and increase the difficulties for lesion localization and segmentation. As a result, image preprocessing has emerged as a crucial step for enhancing the quality of images before segmentation and quantities analysis [3]. Image enhancement techniques are widely employed for increasing the diagnostic quality of dental radiographs. For the most part, Gaussian filtering is a frequently used and effective technique to suppress random noise while maintaining detail in important anatomical or pathological structures. Histogram equalization also redistributes gray-level intensities to improve global contrast of the image and consequently makes it more visible, including the boundaries associated with lesions and surrounding anatomical features. Such preprocessing methods not only represent the image in a more suitable space for subsequent segmentation but also enhance the segmentation performance [4,5]. One of the most important stages of computer-aided diagnosis (CAD) systems is image segmentation, which allows pathological regions to be separated from commensurate healthy tissue. Clustering-based algorithms are ideally appealing among the traditional segmentation methods mainly due to their computational

Vol 14, No 2 (2026) DOI 10.5195/d3000/2026.1548

simplicity and effectiveness. K-means: The K-Means clustering algorithm divides image pixels into separate clusters based on the similarity in intensity, while Fuzzy C-Means (FCM) includes multiple membership values for each pixel, where it may belong to two or more clusters depending on the [6]. Despite several works having made efforts in the field of enhancing and clustering-based segmentation methods for dental radiographs, most of them are limited to evaluating a separate algorithm only. There was limited work in the image enhancement, clustering-based segmentation, and morphological post-processing procedures of an integrated framework to extract lesion information. Additionally, most of the previous studies had focused on qualitative analysis while providing a qualitative assessment of computational efficiency and quantitative evaluation of lesion extraction [7,8]. Various previous studies investigated the automated analysis of dental X-ray images by using classical image processing and clustering methods. Fariza et al. [7] developed a Gaussian kernel-based conditional spatial fuzzy C-means algorithm for tooth component segmentation and demonstrated an enhanced accuracy in segmentation compared to conventional FCM. Ma et al. [7] proposed a segmentation framework based on deep learning for panoramic dental radiographs as an example of how heavily the image preprocessing techniques determine the performance over larger datasets. Some other approaches, similar to what we introduced here, worked independently on improving the histogram-based enhancement and clustering algorithms to obtain better visualization of excessive lesions as well as their segmentation but did not try evaluating all techniques separately or combined together (i.e., image enhancement + clustering-based segmentation + morphological post-processing for the extraction of lesions). Hence, this paper proposes a Gaussian-filtered and histogram-equalized clustering-based segmentation approach with morphological post-processing as a hybrid framework for the lesion segmentation in panoramic dental radiographs. The bunch envisaged an open way of life among us to enable probably the best conceivable lesion extraction by diminishing image noise and bettering the edge areas recognized in skull images, leading to improved segmentation accuracy. A comprehensive method for evaluation between the proposed framework and conventional segmentation methods through quantitative image quality metrics, computational time, and segmentation performance measures is provided to assess its effectiveness in detecting dental lesions.

**Theoretical Spectrum**

**Gaussian Filter**

One of the most widely used linear filters in image processing, the Gaussian filter is mostly employed in context-based noise reduction algorithms, where it must minimize noise while maintaining areas with high structural content. It uses the Gaussian function; based on the distance of the center pixel, a smooth weight is applied that decreases with distance from the center pixel. The Gaussian filter can be implemented as follows, based on the formulation by Deng and Cahill.

$G(x,y)=\frac{1}{2\pi\sigma^2}\exp(\frac{-x^2}{2\sigma^2}+y^2)$…….(1)

Where σ is the standard deviation, which controls how wide or narrow the Gaussian distribution is, and G(x,y) is the point (x,y) of a Gaussian kernel. Parameter σ mostly decides the level of smoothing. σ that is small retains edges and fine structures, leading to a narrower kernel, while larger values help in smoothing strongly, making significant noise reduction possible but blurring edges. The Gaussian filter works on the convolution of an input image with the kernel (Gaussian function). This process creates a weighted average effect by providing larger values (weight) for pixels close to the center and lower ones for those far from it. This yields low-frequency mantle components corresponding to the important aspects of visualization while toning down higher ,frequencies such as noise. In the context of adaptive Gaussian filtering discussed in [2,3], σ is path-dependent and varies with respect to local image characteristics. This enables the filter to obtain a balance between noise suppression and edge preservation by applying stronger smoothing in homogeneous areas and weaker smoothing close to edges [9].

**Image Contrast Enhancement**

Improving Image Contrast: This preprocessing method enhances the quality of an image for a certain use. To emphasize important structures, image augmentation techniques have been used in medical image analysis, particularly in dental radiography. Before further segmentation, the gum disease lesions in this study are contrast-enhanced to differentiate them from nearby normal tissues. The application determines how effective enhancement approaches are, and choosing the right approach frequently necessitates experimental testing.

$S_k$ =T($r_K$)=(L-1)$\sum_{j=0}^{k} p_r\ (r_j)$……(2)

where $r_K$ shows the gray level input., $S_k$ i L represents the entire number of possible intensity levels in the image (usually 256 for 8-bit images), and s is the matching output gray level following transformation. The term$p_r\ (r_j)$ is the gray levels' probability density function (PDF), which is the ratio of the number of pixels with intensity $(r_j)$ and the total number of pixels in the image. The summation term represents the cumulative distribution function (CDF), which accumulates the probabilities of all gray levels up to $(r_j)$. By multiplying the CDF by (L−1), The original intensity values are mapped to a new range that covers the image's whole dynamic range. This leads to a uniform histogram, due to the wide distribution of the most frequently occurring intensity values. This means hidden low contrast zones can come out, and small details are more easily perceptible. In medical and dental X-ray images, the intensity values are limited to a narrow range, which makes high contrast indispensable for detecting structural variations and lesions [10].

**Image Quality**

Image Quality Assessment (IQA) is a fundamental field, which measures the performance of these techniques in enhancement, restoration, and analysis as shown in [1]. It gives two things: one, quantitative measures and perceptual image-matching metrics that tell how much a processed image is like its reference (original) image. This is crucial for applications ranging from medical to scientific imaging, as many IQA methods aim at determining which image processing operations can or cannot be tolerated because they retain or destroy the information. There exist two kinds of VQA methods: perceptual methods that imitate the human visual perception and full-reference methods that require the original image for comparison. As Sonawane et al. state in his 2016 paper "Image Quality Assessment Techniques: An Overview," IQA measures are an important part of it because they provide objective numerical parameters that indicate picture fidelity and visual quality. Similar to this, Sara et al. had the sentence in "Image Quality Assessment using FSIM, SSIM, MSE, and PSNR—A Comparative Study" that many accompanying metrics are usually used to give a precise summary since no solitary metric can properly reflect image quality shows this fact best [11].

**Mean Squared Error (MSE)**

One of the most used full-reference image quality measurements is Mean Squared Error (MSE). This metric provides a straightforward numerical measure of distortion by calculating the mean squared difference between the original and converted images. The definition of MSE is

MSE = 1/(MN) Σ(i=1)^M Σ(j=1)^N [I(i,j) - K(i,j)]². (3)

With M and N being the size of the image, I(i,j) = I_original * K(i,j). That means that the lower the MSE number, the more similar the two

Vol 14, No 2 (2026) DOI 10.5195/d3000/2026.1548

images are, and an MSE=0 means both images are perfectly matched. [12]

**Peak Signal-to-Noise Ratio (PSNR)**

A statistic that is frequently derived from MSE and represented in decibels (dB) is the peak signal-to-noise ratio, or PSNR. It is used to calculate the ratio of the actual distortion noise power to the highest signal strength that can be achieved. The definition of PSNR is

PSNR = 10 $\log_{10}$ [ (L-1)² / MSE ]…… (4)

where L represents the image's potential intensity levels. Greater PSNR values are associated with less distortion and higher image quality. In general, we can consider an image quality to be adequate for most image processing applications if the PSNR is more than 30 dB. [12]

Structural Similarity Index Measure (SSIM)

A perceptual-based metric called the Structural Similarity Index Measure (SSIM) uses contrast, brightness, and structural information to assess the quality of a picture. SSIM is intended to more accurately simulate human visual perception than MSE and PSNR. It is described as:

SSIM(x,y) = $[(2\mu_x\mu_y + C_1)(2\sigma_{xy} + C_2)] / [(\mu_x^2 + \mu_y^2 + C_1)(\sigma_x^2 + \sigma_y^2 + C_2)]$……(5)

Where $\mu_x$ and $\mu_y$ represent the mean intensities of the images, $\sigma x^2$ and $\sigma y^2$ represent variances, $\sigma_{xy}$ is the covariance, and $C_1$ and $C_2$ are small constants used for stability. SSIM values range from -1 to 1, where a value of 1 indicates perfect structural similarity between images [12].

**K-means Clustering Method**

In image processing, K-means clustering is a widely used unsupervised segmentation method that is often used for dental radiographs and other medical imaging [24]. This clustering technique divides picture pixels into K clusters according to feature space or pixel intensity similarity. K-means is successfully used to cluster regions with similar panoramic X-ray image region characteristics in the study "Evaluating the Index of Panoramic X-ray Image Quality Using K-means Clustering Method" (Imago et al.). This results in significant classification of constructing differentiable spatial areas, namely, anatomical structures and important diagnostic areas. The algorithm's foundation is the minimization of an objective function, which is specified as follows and describes the overall within-cluster variance:

$J_{CK} = \sum_{x_i \in c_K} || x_i - u_k ||^2$ ………(6)

The term $J_{CK}$ denotes the cost function of the cluster $c_K$, representing the total within-cluster variance. The symbol $c_K$ refers to the k cluster, which is a group of data points assigned together. Each $x_i$ represents an individual data point within this cluster, such as a pixel or a feature vector in image processing. The term $u_k$ denotes the centroid of the cluster, calculated as the mean of all data points in CK, and serves as the representative point of the cluster. The expression $|| x_i - u_k ||^2$ represents the squared Euclidean distance between the centroid and the data point, indicating the degree to which each point deviates from the cluster center. Finally, the summation $\sum_{x_i \in c_K}$ indicates that this distance is calculated and then aggregated for each point in the cluster [13,14].

**Fuzzy C-Means (FCM)**

The input data is divided into many groups by the fuzzy c-means (FCM) algorithm. The approach made use of the idea of probability. Each data item may concurrently belong to many clusters, with varying degrees of membership determined by a specific membership function, since FCM is a soft clustering technique. The following equation [15] represents the minimization of the objective function J, which is the foundation for FCM's operation:

$J = \sum_{j=1}^{N} \sum_{j=1}^{c} u_{ij}^{m} || x_i - c_j ||^2$ ……….(7)

Where $u_{ij}$ is the degree of the membership, $x_i$ is the data item that belongs to some degree to the cluster j, $cj$ is the cluster seed, and $|| x_i - c_j ||^2$ is the distance between each designated dataset and its corresponding centroid [18]. The dataset is partitioned by iteratively minimizing the objective function. In each round, the membership values $uijm$ of each data item are updated, as well as the clusters' centroids $cj$, as shown in the following equation [16].

**Histogram Equalization**

Image histogram equalization is a classical image processing method for contrast enhancement that can even be used as one of the previous steps to perform an image segmentation problem. It redistributes the intensity values of an image across the full range to make difficult-to-distinguish features in low-contrast images easier to see. While this increase is more significant in medical imaging like dental X-ray processing, it is still necessary where subtle variations of intensity can identify vital diagnostic detail. Because of this nature, histogram equalization can be used to segment regions where the contrast between structures is low, thus aiding segmentation. It obtains a stretching of the intensity distribution, which increases separability (separation between class areas) of the parts, facilitating in this way the performance of methods of subsequent segmentation such as thresholding and clustering algorithms. Histograms are a great way to understand how pixel intensities are distributed in an image, and histogram equalization spreads the values within a narrow range in an image so that tone boundaries between objects begin to pop out more. From a mathematical perspective, histogram equalization is defined based on a transformation function obtained from the CDF of the image histogram:

$s_k$= (L - 1) $\Sigma_{k}^{j=0}$ $p_r(r_j)$………(8)

where $s_k$ represents the output intensity level, L is the number of gray levels, and $p_r(r_j)$ is the probability density function of the input intensity levels. This transformation maps the original intensity values into a new range that enhances global contrast [17].

**Hybrid Technique**

The proposed hybrid technique combines histogram equalization with fuzzy C-means (FCM) clustering to improve lesion segmentation in panoramic dental X-ray images. As illustrated in Figure 1, histogram equalization is first applied as a preprocessing step to enhance the global image contrast by redistributing the gray-level intensity values. This enhancement increases the visibility of lesion boundaries and facilitates the separation of pathological regions from surrounding tissues. After image enhancement, the processed image is segmented using the Fuzzy C-Means (FCM) clustering algorithm. Unlike hard clustering methods, FCM assigns each pixel a degree of membership to multiple clusters, allowing more accurate segmentation of lesions with unclear or irregular boundaries. The improved contrast produced by histogram equalization enables FCM to classify image pixels more effectively, resulting in better localization of the lesion region. Finally, morphological operations are applied to eliminate small, isolated regions, remove noise, and smooth the segmented lesion boundaries. The integration of histogram equalization with FCM reduces the computational complexity of the clustering process while improving segmentation accuracy and producing more reliable lesion extraction results compared with the individual segmentation methods.

## Material and Methods

This work explores dental X-ray images and localizes gum lesions through several techniques for image processing. In the proposed methodology, segmentation is next after image extent. Image Quality Evaluation Image quality enhancement is achieved by several contrast enhancement techniques such as applying Gaussian filtering, histogram equalization, and contrast adjustment followed by evaluation metrics. The enhanced image is further segmented into relevant segments by different methods: K-means, fuzzy C-means (FCM) clustering, histogram-based techniques, and histogram equalization. Various methods are used in this research here to decrease the calculation time and improve segmentation quality. Several

Vol 14, No 2 (2026) DOI 10.5195/d3000/2026.1548

hybrid methods have been used that cluster on FCM and histogram equalization. To verify the accuracy of the proposed method, segmentation results were compared to doctor annotations by highlighting the area in question and further refining these findings using morphological operators as well as measuring the lesion size. Figure 1 depicts the preprocessing, segmentation, and post-processing phases of the suggested lesion segmentation framework's total workflow.

In this work, expert delineation of lesion locations provides the reference standard for assessments, effectively creating a baseline against which performance can be compared. This division enables the comparison of results of models proposed for finding lesions and measurements in areas where these tumors appear. The experimental dataset includes a total of five dental X-rays that show the locations of gum lesions overlaid on them. These images are applied to the segmentation and enhancement approaches we propose. In the following section, we provide a detailed summary of the data set image quality, acquisition source, and size.

## Results and Discussion

This section presents the outcomes of the three approaches used to identify, segment, and extract the impacted regions, as well as the augmentation techniques.

### Pre-Processing

### Region of Interest (ROI) Step

Cutting the image background and eliminating any excess material is the initial stage in this process. The outcomes of this procedure for the lung lesion images are shown in Figure 2.

### Enhancement Image Step

Second step, Image Quality Enhancement. Firstly, the images are enhanced using a Gaussian filter, followed by contrast adjustment. The enhanced images are then displayed in Figure 3.

### Image Quality Evaluation

Three commonly used metrics—mean squared error (MSE), peak signal-to-noise ratio (PSNR), and structural similarity index (SSIM)—were utilized to assess the suggested image processing technique. These metrics were calculated to measure the improvement in image quality that results from applying contrast enhancement and Gaussian filtering (Table 2).

The quality criteria are displayed in the table. The Gaussian filter is represented by the letter (G), and the contrast adjustment method is represented by the letter (C). The Mean Squared Error (MSE), Maximum Signal-to-Noise Ratio (PSNR), and Structural Similarity Identity (SSIM) criteria were used to assess the effectiveness of both approaches. The Gaussian filter's MSE values were extremely low, ranging from 0.000372 to 0.00060033, showing a high level of image content preservation effectiveness. The high PSNR values, which varied from 32.2161 dB to 39.8504 dB, indicate excellent image quality and minimal processing-related distortion. The SSIM values, which are near to one and range from 0.8789 to 0.9803, show that the processed images preserve the fundamental details and structure of the original image. The MSE values for the contrast adjustment technique ranged from 0.0018 to 0.0031. These values are higher than those for the Gaussian filter, suggesting that the image changed more after processing. The PSNR values were lower than those attained using the Gaussian filter, ranging from 25.0913 dB to 27.3701 dB. The SSIM values, on the other hand, showed good preservation of the image's structural similarity, ranging from 0.9082 to 0.9727. According to the results, the contrast adjustment strategy demonstrated good SSIM values, but the Gaussian filter outperformed it in terms of both MSE and PSNR, obtaining the lowest error rate and the maximum image quality. Thus, in this investigation, the Gaussian filter can be regarded as the most effective technique for improving and maintaining image quality.

### K-Means Clustering Method

The K-means algorithm was used to cluster the upgraded dental X-ray images using two distinct k values (4 and 5) for segmentation. To assess how well the technique separated lesion regions from surrounding tissue, several cluster values were chosen. The segmented images show how the clusters affect the lesion detection quality. The outcomes of this approach are summarized in Figures 4 and 5.

In Figures 4 and 5, column (a) represents the enhanced image input into the processing system, while column (b) represents the image after applying K-means clustering. Column (c) shows the cluster containing the lesion, and column (d) represents the extracted lesion region obtained after applying several morphological operations. Five clusters (K = 5) were chosen for the first three photos since choosing K = 3 or K = 4, where the lesion was largely blended with the surrounding backdrop, made it difficult to detect the lesion boundaries. Over-segmentation occurred when the number of clusters was increased to K ≥ 6, which reduced the real size of the lesion and caused it to fracture into smaller sections. On the other hand, four clusters (K = 4) yielded the most accurate segmentation for the fourth image, whereas K = 3 was unable to sufficiently distinguish the lesion from the background, and K ≥ 5 resulted in over-segmentation and partial lesion fragmentation. Consequently, the ideal number of clusters changed depending on the features of each image; for the first three images, K = 5 was ideal, and for the fourth image, K = 4 produced the best segmentation outcome.

### Fuzzy C-Means Segmentation

Fuzzy C-Means (FCM) clustering was applied using several clusters (k = 4) to segment the experimental images and evaluate the optimal separation of regions. Figures 6 and 7 present the corresponding segmentation results obtained from this step.

In Figures 6 and 7, column (a) is the enhanced image to be processed as input to our system, and column (b) gives the output after fuzzy C-means (FCM). Column (c) corresponds to the cluster that contains the lesion, and column (d) is bitwise stripped-out target area post-morphological application. Cluster Type: Results for the first three images show that K = 4 produced the highest accuracy for lesion segmentation, as K = 3 failed to separate the lesions from the surrounding background. On the other end, using (K ≥ 5) clusters yielded over-segmentation as well, leading to a lesion being split into several regions connected in between and with the background. Conversely, for the fourth image, five clusters (K = 5) yielded the ideal segmentation result, but K = 4 could only partially distinguish the lesion from surrounding tissues, and all higher cluster numbers resulted in over-segmentation. These results suggest that the optimal number of clusters depends on the image properties and lesion characteristics; K = 4 fits better to three out of four images, while K = 5 fits better to one image.

### Histogram-Based Segmentation Results

To improve the visibility and extraction of the damaged area, histogram equalization was used as a segmentation technique to increase the contrast between the lesion region and surrounding tissues. Figure 8 presents the corresponding segmentation results obtained from this step.

In Figure 8, column (a) represents the enhanced image input into the processing system, while column (b) represents the image after histogram equalization. Column (c) shows the region corresponding to the affected area following the segmentation process using Otsu's automatic thresholding method (gray thresh), whereas column (d) depicts the affected area after the application of several morphological operations to eliminate small artifacts and refine the lesion boundaries.

### Hybrid Technique

Vol 14, No 2 (2026) DOI 10.5195/d3000/2026.1548

In this paper, we describe a hybrid image segmentation method based on histogram equalization and Fuzzy C-Means (FCM) clustering. Initially, contrast is increased on the whole image with histogram equalization, and the lesion region becomes more visible. This augmented image is then fed into the FCM for image segmentation. For the first three images, 4 clusters were chosen because they showed the best separation of lesion and background. However, the fourth image required five clusters to create a more accurate representation of the lesion since fewer clusters did not separate the lesion from surrounding tissues. Post-processing of the lesion cluster using morphological operations for small artifact covering and better boundary continuity. The proficiently performed hybrid technique integrates image enhancement with fuzzy clustering by outperforming the conventional methods to extract lesions while saving time for processing time. Figures 9 and 10 display the segmentation results of the proposed hybrid technique.

The area ratio of the affected region for each image was determined by calculating the area of the extracted region. This process involved calculating the full area of the lesion extracted via segmentation methods; Table 3 presents the calculated surface area for the lesion images.

The lesion region was extracted by applying a series of morphological operations. Initially, "Opening" and "Closing" operations were performed using structuring elements ranging from 2 to 4 pixels in size to remove small, unwanted objects. Subsequently, a "Small Object Removal" process was applied to eliminate noise and insignificant regions. Finally, the lesion region was isolated and extracted to obtain a precise representation of the lesion, thereby improving segmentation quality and enhancing the efficiency of subsequent analysis stages.

**Manual Radiologist Delineation**

All images under study were manually segmented by a radiologist. The segmented regions were extracted, and their surface areas were calculated to serve as ground truth for evaluating the performance of the implemented segmentation methods. Figures 11 illustrate the results of this step for dental images containing lesions.

The calculated surface area for the areas specified by the dentist is presented in Table 4. The surface area of the lesion sites that the radiologist manually recognized is shown in Table 4. The performance of the suggested segmentation techniques was assessed using these measures as the ground truth, and the relative difference between the segmented findings and the manually recognized lesions was computed. The percent relative differences of the surface area for the extracted abnormal regions for tumors concerning the radiologist delineation were calculated according to the equation:

$$present\ relative\ difference = \frac{|area\ of\ radiologist - area\ of\ implemented\ methods|}{area\ of\ radiologist}$$

The results of this step are presented in Table 5.

The percentage of relative deviations between the reference areas manually drawn by the radiologist and the lesion areas recovered by the applied algorithms is shown in Table 5. The findings show that all approaches yielded very minor variations, indicating strong agreement with the radiologist's observations. In most cases, the Fuzzy C-Means algorithm produced the smallest relative differences among the assessed techniques, whereas the hybrid approach showed somewhat larger discrepancies. The efficacy of the suggested segmentation techniques for lesion extraction from panoramic dental radiographs is generally confirmed by the low percentage results.

The computing time needed for lesion segmentation using the suggested hybrid approach and the traditional Fuzzy C-Means (FCM) technique is contrasted in Table 6. The findings demonstrate that for every examined image, the suggested hybrid approach consistently needed less processing time than the traditional FCM algorithm. The use of histogram equalization prior to the clustering stage, which improves the distribution of intensity values and increases image contrast, is responsible for the decrease in processing time. These findings show that the suggested hybrid architecture increases computing efficiency while maintaining acceptable segmentation performance.

## Conclusion

This study used segmentation approaches based on thresholding and clustering to propose an efficient framework for extracting lesion patches from X-ray images. Following several preprocessing steps, such as image cropping, Gaussian filtering, and contrast adjustment, the proposed methodology used four techniques for lesion segmentation: K-means clustering, Fuzzy C-Means (FCM), histogram equalization, and a hybrid approach that combined Fuzzy C-Means and histogram equalization. Morphological methods were then used to precisely extract the lesion area, delete extraneous regions, and remove noise. Image quality assessment findings revealed that the preprocessing stage effectively contributed to boosting image quality, demonstrating noise reduction while keeping the features and anatomical structures needed for the segmentation procedure. Comparative results further indicated that the hybrid method achieved the best performance among all the methods studied, recording the lowest relative difference, 0.08%, when comparing the largest lesion area against the physician's reference delineation, while maintaining high accuracy across the remaining images. Furthermore, the hybrid approach struck a compromise between computational efficiency and result quality by achieving a notable reduction in execution time when compared to the conventional fuzzy C-means algorithm while maintaining a high degree of segmentation accuracy. Based on the collected results. It can be concluded that integrating contrast enhancement techniques with clustering algorithms, followed by morphological processing, provides a robust and effective framework for extracting lesion regions in X-ray images. Furthermore, the proposed methodology holds significant potential to support computer-aided diagnosis systems by improving the accuracy, consistency, and efficiency of lesion detection in X-ray images.

**References**


[1] White, S. C., & Pharoah Michael, J. (2012). *Oral radiology: principles and interpretation*. Elsevier.

[2] Scarfe, W. C., & Mallya, S. M. (2024). Computed tomography. *White and Pharoah's Oral Radiology-E-BOOK: White and Pharoah's Oral Radiology-E-BOOK*, 156.

[3] Khan, A., Sohail, A., Zahoora, U., & Qureshi, A. S. (2020). A survey of the recent architectures of deep convolutional neural networks: A. Khan et al. *Artificial Intelligence Review*, *53*(8), 5455–5516.

[4] Fariza, A., Arifin, A. Z., Astuti, E. R., & Kurita, T. (2018). Segmenting tooth components in dental x-ray images using a Gaussian kernel-based conditional spatial Fuzzy C-Means clustering algorithm. *International Journal of Intelligent Engineering & Systems*, *12*(3), 108–117.

[5] Zuiderveld, K. (1994). Contrast Limited Adaptive Histogram Equalization. In: Graphics Gems IV. Academic Press.

[6] Bezdek, J. C. (2013). *Pattern recognition with fuzzy objective function algorithms*. Springer Science & Business Media.

[7] Fariza, A., Arifin, A. Z., Astuti, E. R., & Kurita, T. (2018). Segmenting tooth components in dental x-ray images using Gaussian kernel-based conditional spatial Fuzzy C-Means clustering algorithm. *International Journal of Intelligent Engineering & Systems*, *12*(3), 108–117.

[8] Bonfanti-Gris, M., Herrera, A., Salido Rodríguez-Manzaneque, M. P., Martínez-Rus, F., & Pradies, G. (2025). Deep learning for tooth detection and segmentation in panoramic

Vol 14, No 2 (2026) DOI 10.5195/d3000/2026.1548

radiographs: A systematic review and meta-analysis. *BMC Oral Health*, *25*(1), 1280.
[9] Li, H., & Xu, K. (2025). Innovative adaptive edge detection for noisy images using wavelet and Gaussian method. *Scientific Reports*, *15*(1), 5838.
[10] Rivera-Aguilar, B. A., Cuevas, E., Pérez, M., Camarena, O., & Rodríguez, A. (2024). A new histogram equalization technique for contrast enhancement of grayscale images using the differential evolution algorithm. *Neural Computing and Applications*, *36*(20), 12029–12045.
[11] Jamil, S. (2024). Review of image quality assessment methods for compressed images. *Journal of Imaging*, *10*(5), 113.
[12] Sara, U., Akter, M., & Uddin, M. S. (2019). Image quality assessment through FSIM, SSIM, MSE and PSNR—a comparative study. *Journal of Computer and Communications*, *7*(3), 8–18.
[13] Imajo, S., Tanabe, Y., Nakamura, N., Honda, M., & Kuroda, M. (2024). Evaluating the index of panoramic X-ray image quality using the K-means clustering method. *Egyptian Journal of Radiology and Nuclear Medicine*, *55*(1), 4.
[14] Fariza, A., Arifin, A. Z., Astuti, E. R., & Kurita, T. (2018). Segmenting tooth components in dental x-ray images using Gaussian kernel-based conditional spatial Fuzzy C-Means clustering algorithm. *International Journal of Intelligent Engineering & Systems*, *12*(3), 108–117.
[15] Awosina, P. T., Olukanmi, P. O., & Bokoro, P. N. (2026). Comparative Analysis of Clustering Algorithms for Unsupervised Segmentation of Dental Radiographs. *Applied Sciences*, *16*(1), 540.
[16] Koundal, A., Budhiraja, S., & Agrawal, S. (2024). Medical Image Segmentation using Enhanced Feature Weight Learning Based FCM Clustering. *Biomedical & Pharmacology Journal*, *17*, 2661–2672.
[17] Nia, S. N., & Shih, F. Y. (2024). Medical X-ray image enhancement using global contrast-limited adaptive histogram equalization. *International Journal of Pattern Recognition and Artificial Intelligence*, *38*(12), 2457010.

.

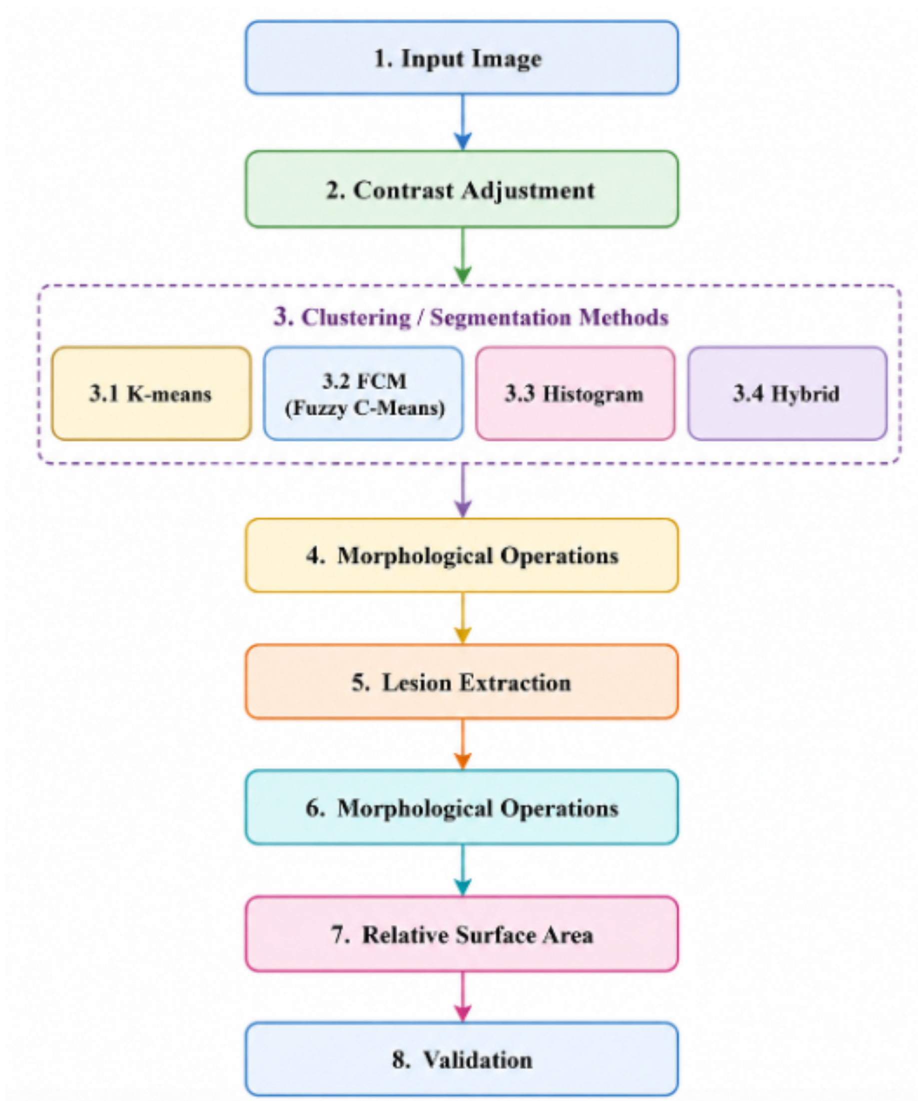


Figure 1. Block diagram of the proposed work.

Vol 14, No 2 (2026) DOI 10.5195/d3000/2026.1548

Table 1. Description of the adopted dental X-ray images, including lesion type, acquisition source, and image size.

| | Name of image | Image size | Abnormaliy type | source |
|---|---|---|---|---|
|  | Image 1 | 2394x1206 | Dental lesion | Emaar dental clinics |
|  | Image 2 | 2394x1206 | Dental lesion | |
| 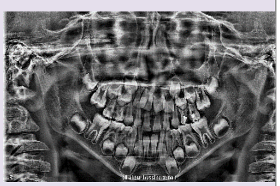 | Image 3 | 2394x1206 | Dental lesion | |
|  | Image 4 | 1554x1004 | Dental lesion | Kaggle Dataset |

Vol 14, No 2 (2026) DOI 10.5195/d3000/2026.1548

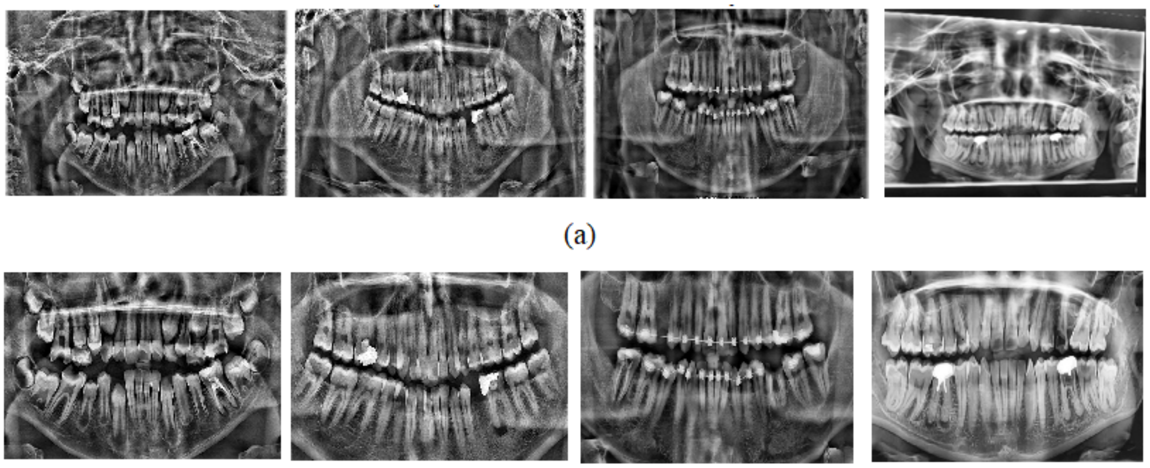

(a)

(b)

Figure 2. Input images of dental x-ray: (a) before background cutting, (b) after background cutting and removing any extra parts.

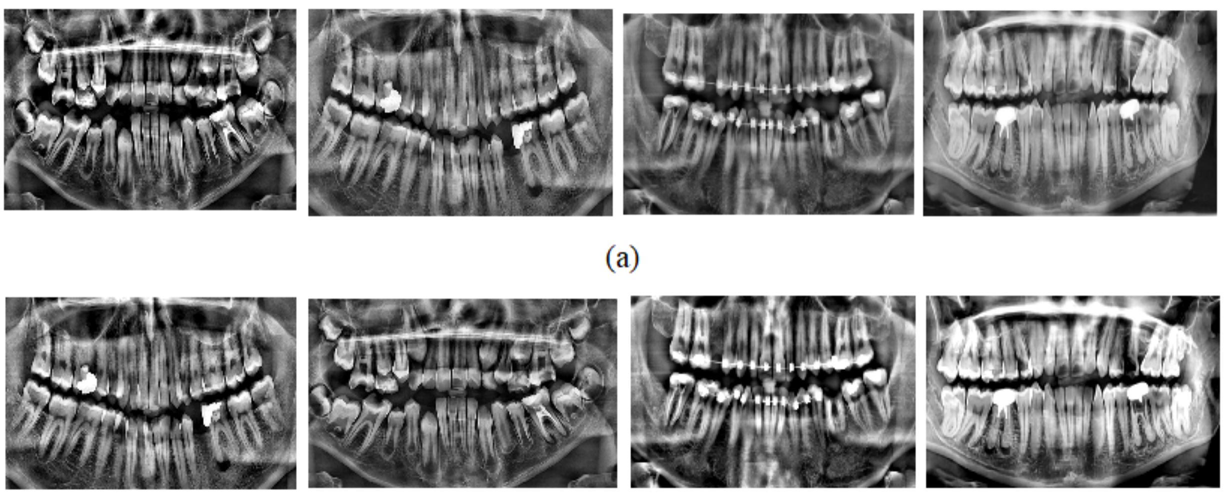

(a)

(b)

Figure 3 displays the lesion's dental X-ray images: (a) shows the image after the Gaussian filter was applied, and (b) shows the picture after contrast adjustment.

Table 2. Image quality metrics for Gaussian filter and contrast enhancement.

| Image | MSE (G) | PSNR (G) | SSIM (G) | MSE (C) | PSNR (C) | SSIM (C) |
|---|---|---|---|---|---|---|
| Lesion 1 | 0.00051218 | 32.9058 | 0.9041 | 0.0024 | 26.2757 | 0.9082 |
| Lesion 2 | 0.00060033 | 36.2161 | 0.8789 | 0.0018 | 27.3701 | 0.9416 |
| Lesion 3 | 0.00052964 | 32.7602 | 0.9339 | 0.0028 | 25.5368 | 0.9727 |
| Lesion 4 | 0.00037272 | 39.8504 | 0.9803 | 0.0031 | 26.0913 | 0.9572 |

Vol 14, No 2 (2026) DOI 10.5195/d3000/2026.1548

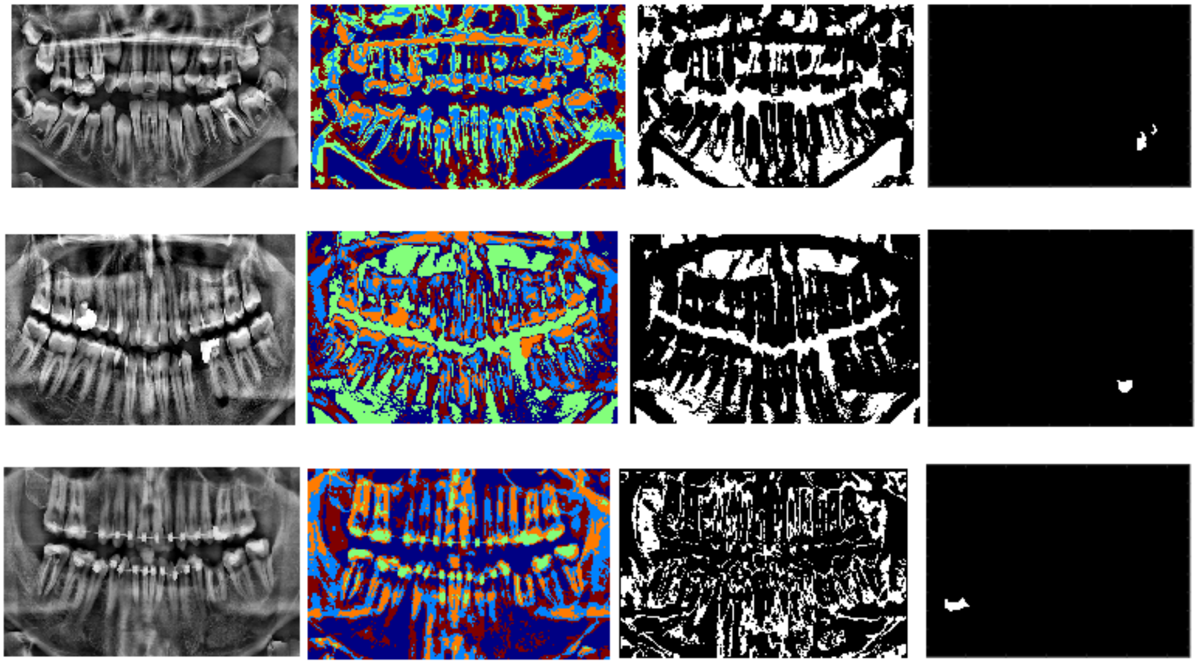

(a) (b) (c) (d)

Figure 4. Results of implementing K-means clustering with five clusters. (a) enhanced image, (b) image after applying the K-means algorithm, (c) the cluster of the infected region, and (d) the final extracted infected region.

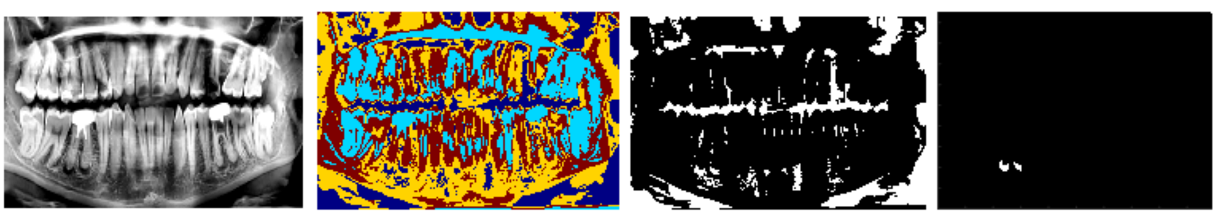

(a) (b) (c) (d)

Figure 5. Results of implementing K-means clustering with four clusters: (a) enhanced image, (b) image after applying the K-means algorithm, (c) the cluster of the infected region, and (d) the final extracted infected region.

Vol 14, No 2 (2026) DOI 10.5195/d3000/2026.1548

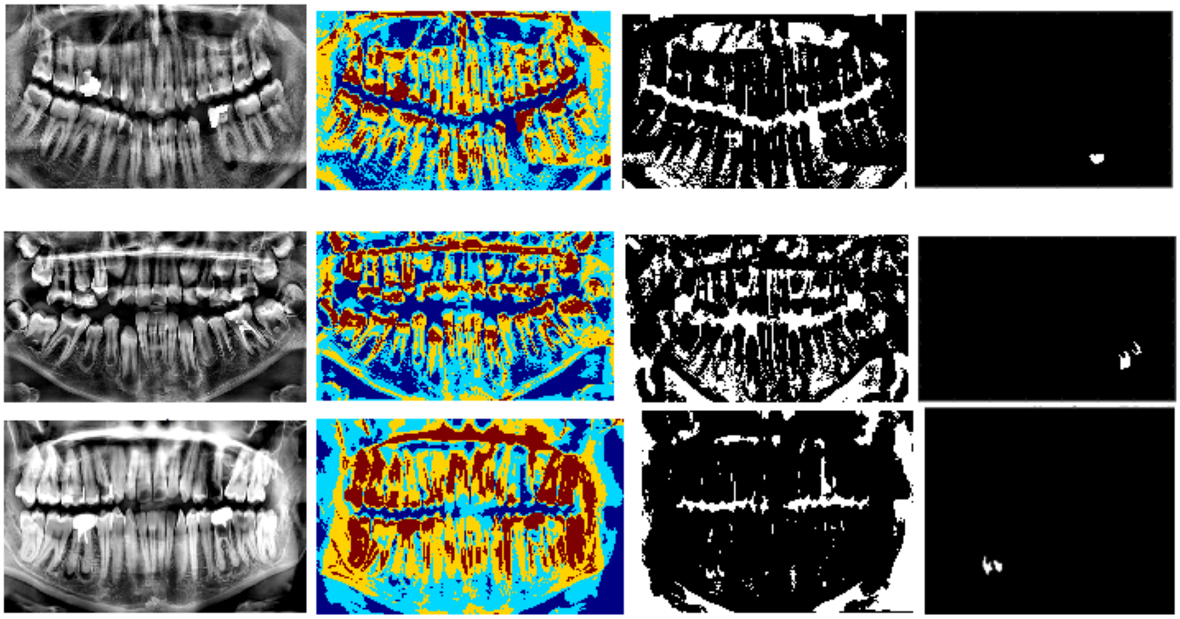

(a) (b) (c) ( d)

Figure 6. Results of implementing FCM clustering with four clusters: (a) enhanced image, (b) image after applying FCM, (c) the cluster of the infected region, and (d) the final extracted infected region.

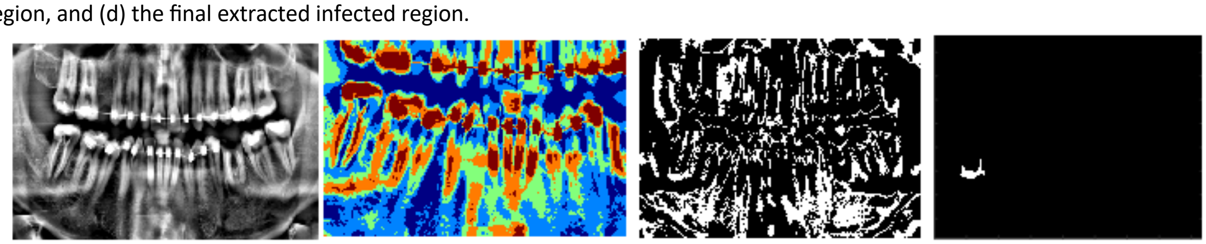

(a) (b) (c) ( d)

Figure 7. Results of implementing FCM clustering with five clusters. (a) enhanced image, (b) image after applying FCM, (c) the cluster of the infected region and (d) the final extracted infected region.

Vol 14, No 2 (2026) DOI 10.5195/d3000/2026.1548

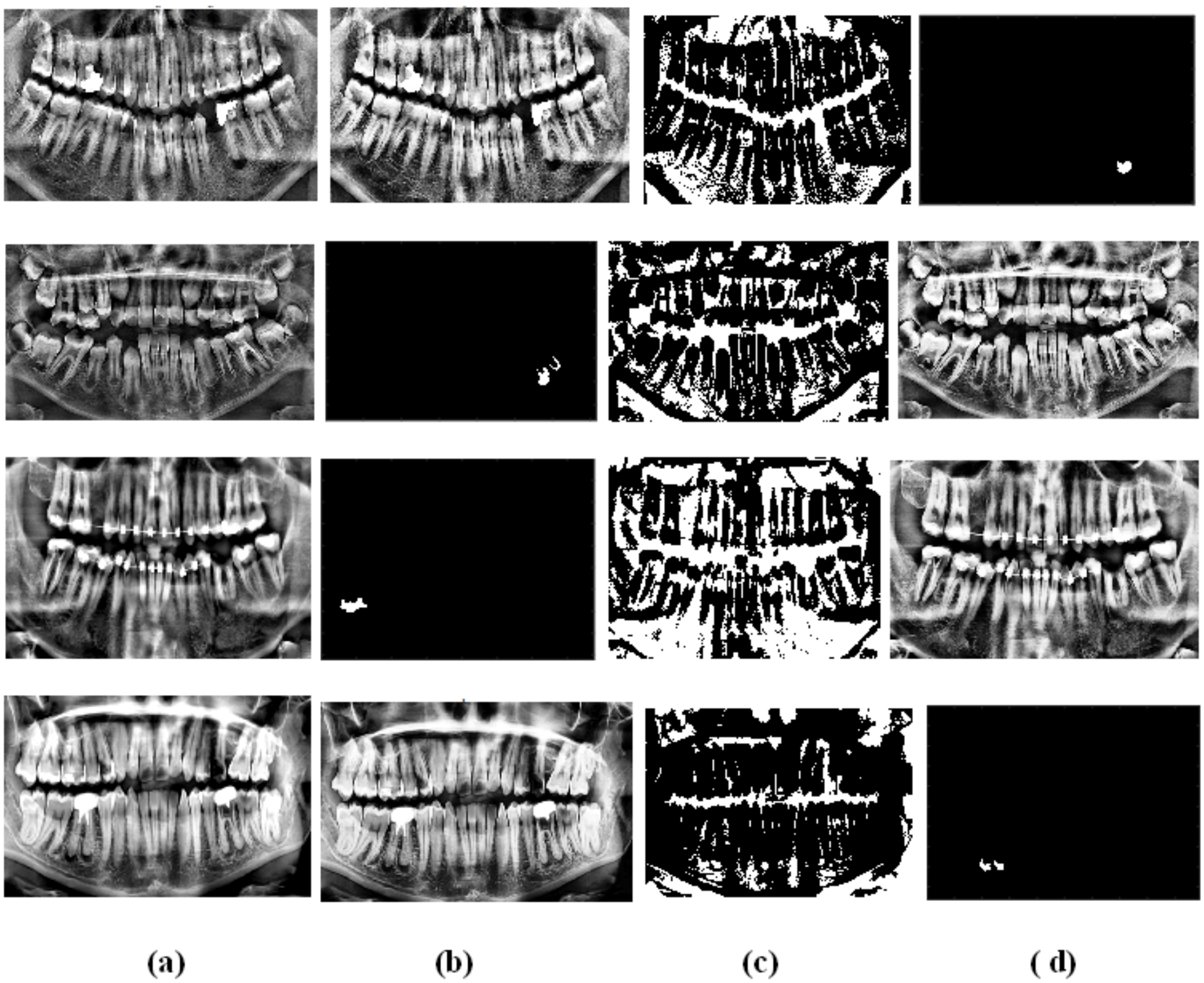


Figure 8. Segmentation of the lesion region using histogram-based intensity separation.

Vol 14, No 2 (2026) DOI 10.5195/d3000/2026.1548

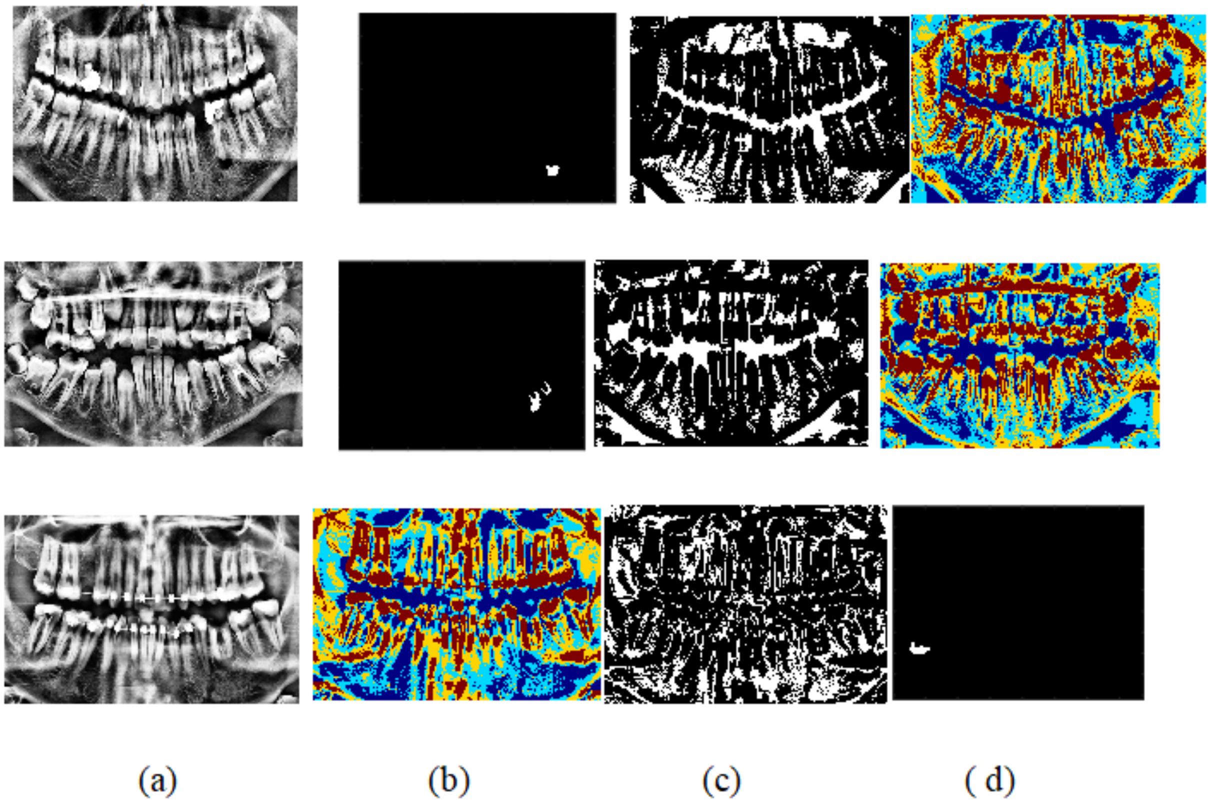


Figure 9. Results of applying hybrid clustering with four clusters. (a) Image after histogram equalization; (b) after applying Fuzzy C-Means; (c) the cluster containing the lesion; (d) the finally extracted affected region.

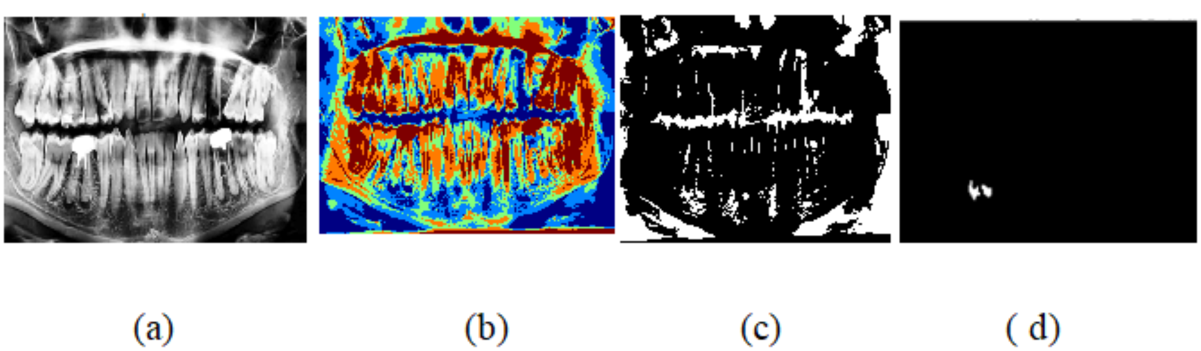


Figure 10. Results of implementing hybrid clustering with five clusters. (a) Image after histogram equalization; (b) after applying Fuzzy C-Means; (c) the cluster containing the lesion; (d) the finally extracted affected region.

Table 3. Calculated surface area for the specified regions using the employed methods.

| Images | k-means | FCM | histogram equaliza-tion | Hybrid |
|---|---|---|---|---|
| Lesion1 | 1086 | 1077 | 1085 | 1082 |
| Lesion2 | 861 | 862 | 870 | 863 |
| Lesion3 | 1884 | 1888 | 1901 | 1899 |
| Lesion4 | 1159 | 1152 | 11608 | 1158 |

Vol 14, No 2 (2026) DOI 10.5195/d3000/2026.1548

Figure 11. Physician's identification of the lesion areas following the application of certain image processing functions.

Table 4. Calculated surface area for the areas identified by the dentist.

| Calculated surface area of the areas specified by the dentist (pixels) | | | |
|---|---|---|---|
| Les1 | Les2 | Les3 | Les4 |
| 1080 | 865 | 1896 | 1157 |

Table 5. Percentages of relative differences for the extracted lesion when applying the proposed methods versus boundary delineation by a radiologist.

| percent Relative Differences (%) | | | | |
|---|---|---|---|---|
| Images | k-means (%) | FCM (%) | histogram equalization (%) | Hybrid (%) |
| Les 1 | 0.47 | 0.27 | 0.55 | 0.18 |
| Les 2 | 0.46 | 0.34 | 0.57 | 0.23 |
| Les 3 | 0.63 | 0.42 | 0.85 | 0.15 |
| Les 4 | 0.17 | 0.43 | 0.95 | 0.08 |

Table 6. The elapsed time and the percent relative reduction time of the hybrid technique for images.

| Images | FCM Time (s) | Hybrid Method Time (s) |
|---|---|---|
| Les1 | 47.845384 | 18.583824 |
| Les2 | 46.23721 | 27.637052 |
| Les3 | 49.23721 | 9.1351853 |
| Les4 | 33.247834 | 13.363462 |